Lithium-Ion Batteries

International Edition: DOI: 10.1002/anie.201503072
German Edition: DOI: 10.1002/ange.201503072

Pushing Up Lithium Storage through Nanostructured Polyazaacene Analogues as Anode**

Jiansheng Wu, Xianhong Rui, Guankui Long, Wangqiao Chen, Qingyu Yan, and Qichun Zhang**

Abstract: *According to the evidence from both theoretical calculations and experimental findings, conjugated ladder polymers containing large π-conjugated structure, a high number of nitrogen heteroatoms, and a multiring aromatic system, could be an ideal organic anode candidate for lithium-ion batteries (LIBs). In this report, we demonstrated that the nanostructured polyazaacene analogue poly(1,6-dihydropyrazino[2,3g]quinoxaline-2,3,8-triyl-7-(2H)-ylidene-7,8-dimethylidene) (PQL) shows high performance as anode materials in LIBs: high capacity (1750 mAh g^{-1}, 0.05C), good rate performance (303 mAh g^{-1}, 5C), and excellent cycle life (1000 cycles), especially at high temperature of 50°C. Our results suggest nanostructured conjugated ladder polymers could be alternative electrode materials for the practical application of LIBs.*

Although rechargeable lithium-ion batteries (LIBs) have been widely used as the power source for portable electronics, they still cannot meet the emerging requirements in high-energy and high-power applications such as plug-in electrical vehicles (EVs) and hybrid electrical vehicles (HEVs).[1] Thus, developing new electrode materials, which can deliver higher capacities with high cycling stabilities when they are charged/discharged at high currents, is highly desirable.[2]

To address these issues, many redox-active inorganic electrode materials including transition metal oxides, metals, and their alloys have been strongly investigated.[3] Although these materials have been predicted to show very high theoretical Li intercalation capacity compared with that of commercially used electrode materials, the practical lithiation process in most of these materials is affected by the significant volume expansion (up to 150%), which could cause the pulverization of the materials and lead to the poor charge/discharge cycling performances. Even though some improvements on the cycle ability and specific capacity have been approached through materials nanoengineering, the preservation of high capacities after numerous charge/discharge cycles is very challenging due to the nanoparticles' aggregation and their structural collapse during the insertion or extraction of Li ions. Therefore, searching novel alterative materials to solve current problems in LIBs is urgent.[4]

Organic compounds could be promising candidates for electrode materials because they have been widely considered as promising candidates to construct flexible, stretchable, low-cost, and potentially high-capacity LIBs.[5] Moreover, organic synthesis could allow scientists to tune materials properties through structural control and the selection of functional groups. Current research on organic electrode materials mainly focus on organodisulfides,[6] nitroxyl radical polymers,[7] semiconducting polymers,[8] organic salts,[9] and conjugated carbonyl compounds (e.g., quinones and tetracarboxylic dianhydrides).[10] Although some of them have already shown promising electrochemical performance, such applications are limited to cathodes rather than anodes owing to their relatively high redox potentials (typically 1.5–4.0 V vs. Li^+/Li). Moreover, the LIB applications of nanostructured organic materials still remain unexplored. Reports in literature are still rare and our ability to design high-efficient organic materials that may achieve large specific capacities at very high current densities is still limited.

Recently, organic polymers with a stable skeleton have been proven to be an efficient strategy to address these problems, because they are completely insoluble in organic electrolytes. Moreover, their performance could be further enhanced through nanoengineering. On the other hand, each benzene ring in a conjugated system can reversibly accept 6 Li ions to form a Li6/C6 complex.[11] If heteroatoms are introduced to conjugated organic systems, redox reactions are more likely to occur on the center with lone pair electrons (e.g., O, N).[12] These experimental results coupled with the theoretical calculations indicate that multiring aromatic systems with heteroatom "doping" could be a promising alternative.

Our group has been working on oligoazaacenes for a long time.[13] Oligoazaacenes are electron-deficient systems and

[*] Dr. X. Rui[+]
School of Energy and Environment, Anhui University of Technology
Anhui 243002 (China)
Dr. J. Wu,[+] Dr. X. Rui,[+] Dr. G. Long, W. Chen, Prof. Q. Yan, Prof. Q. Zhang
School of Materials Science and Engineering
Nanyang Technological University
Singapore 639798 (Singapore)
E-mail: alexyan@ntu.edu.sg
qczhang@ntu.edu.sg
Prof. Q. Zhang
Division of Chemistry and Biological Chemistry
School of Physical and Mathematical Sciences
Nanyang Technological University
Singapore 637371 (Singapore)
[+] These authors contributed equally to this work.

[**] Q.Z. acknowledges financial support from AcRF Tier 1 (RG 16/12) and Tier 2 (ARC 20/12 and ARC 2/13) from MOE, and the CREATE program (Nanomaterials for Energy and Water Management) from NRF, Singapore. Q.Y. acknowledges Singapore MOE AcRF Tier 1 grants (RG2/13), and the Singapore National Research Foundation under CREATE program: EMobility in Megacities.

Supporting information for this article is available on the WWW under http://dx.doi.org/10.1002/anie.201503072.

the solubility deteriorates with the increasing length. In addition, we also found that nanostructured poly(benzobisimidazo benzophenanthroline) showed excellent electrochemical performance as anode material for LIBs.[14] This knowledge strongly encouraged us to prepare the polyazaacene analogue poly(1,6-dihydropyrazino[2,3g]quinoxaline-2,3,8-triyl-7-(2*H*)-ylidene-7,8-dimethylidene) (PQL), which exhibits a large π-conjugated structure, a high number of nitrogen heteroatoms, and a multiring aromatic system. Such a material should be an ideal organic anode candidate for LIBs.

The PQL was prepared by the reaction between 2,5-dihydroxy-1,4-benzoquinone and 1,2,4,5-tetraaminobenzene tetrahydrobromide (TAB·4 HBr) in 116% polyphosphoric acid (PPA) at 190 °C for 10 h (Scheme 1).[15] The nanoparticles of PQL were fabricated by dissolving PQL in methanesulfonic acid (MSA), followed by reprecipitation with water. The centrifuge-separated, washed, and dried particles were used as anode materials for rechargeable LIBs.

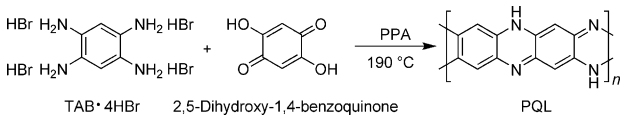

Scheme 1. Synthesis of the ladder polymer PQL.

The as-prepared pristine PQL and PQL nanoparticles were characterized by Fourier transform infrared (FTIR) spectroscopy (Figure 1 a). In agreement with previous reports for pristine PQL,[16] the absorption peak observed around 3300 cm^{-1} was due to N–H stretching vibrations. The absorption peaks in the range of 1612–1250 cm^{-1} can be assigned to the stretching vibrations of the C=N and C–N bonds whereas the peak at 840 cm^{-1} is associated with the skeletal vibrations of the phenazine ring. In the spectrum of partly doped PQL nanoparticles, the stronger absorption peaks at 1460 and 840 cm^{-1} are due to the increased vibrations of C=N and the phenazine ring, indicating the enhanced conjugated structure of the PQL main chain.[16] The results are also verified by electrical conductivity measurements. The conductivity of pristine PQL and PQL nanoparticles was measured by the four-point method and found to be 1×10^{-5} S cm^{-1} and 2.1×10^{-3} S cm^{-1}, respectively. XRD patterns of pristine PQL and PQL nanoparticles are shown in Figure 1 b. Two small board peaks around 10° and 27° suggest the weak crystallinity of both materials. The similar FTIR and XRD results indicated that the structure of PQL has no change after nanoengineering. As shown in Figure S1, pristine PQL is largely aggregated, whereas after reprecipitation, PQL formed nanoparticles (Figure 2). The diameter of PQL

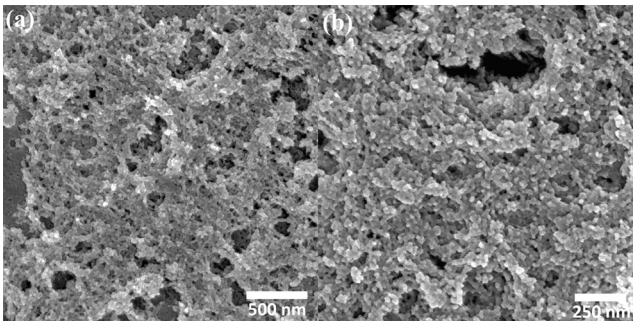

Figure 2. FESEM images of PQL nanoparticles. a) Low-resolution micrograph of the large quantity of PQL nanoparticles. b) High-resolution image of PQL nanoparticles.

nanoparticles is about 40–60 nm. The thermal stability of PQL nanoparticles was also investigated. As shown in TGA curves (Figure S2), the PQL nanoparticles display a very good thermal stability ($\approx$400 °C) in air, which indicates that PQL could be used as an electrode material at high temperature.

The electrochemical performance of PQL nanoparticles was evaluated in comparison with lithium metal in coin-type cells. To investigate the redox behavior of PQL, the cyclic voltammetry (CV) measurement was initially performed in the voltage range of 0.0–3.0 V at a scan rate of 0.1 mV s^{-1} at ambient temperature (ca. 25 °C), as shown in Figure 3 a. Notably, there are some differences in the CV curves (especially for the lithiation brand) between the first and subsequent cycles. During the first cathodic scan, the peak at around 1.4 V can be attributed to the addition of lithium to nitrogen atoms and the occurrence of some side reactions (e.g., the removal of H atoms from sp^3 N centers). The discharge (lithiation) completed with a sharp current declination from 0.8 V is ascribed to Li^+ ion intercalation into C_6 aromatic rings and the formation of a solid electrolyte interphase (SEI) film at the electrode–electrolyte interface. On the reverse charge sweep, a current hump starting at ca. 0.1 V and extending to about 1.6 V is investigated, corresponding to the extraction processes of Li^+ ions from lithiated PQL step by step. From the second cycle onwards, the CV curves almost overlap, indicating the stable and superior

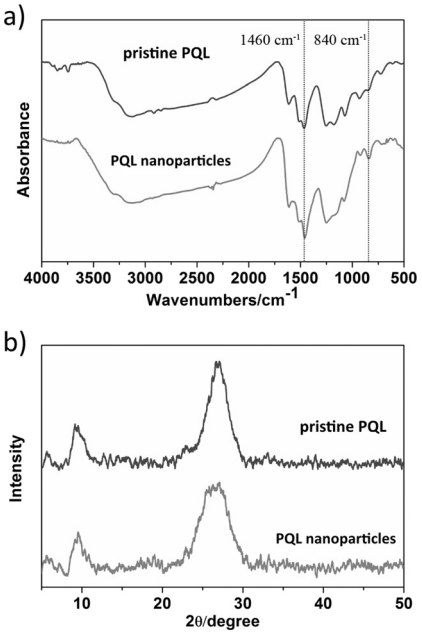

Figure 1. a) FTIR spectra and b) XRD patterns of PQL.

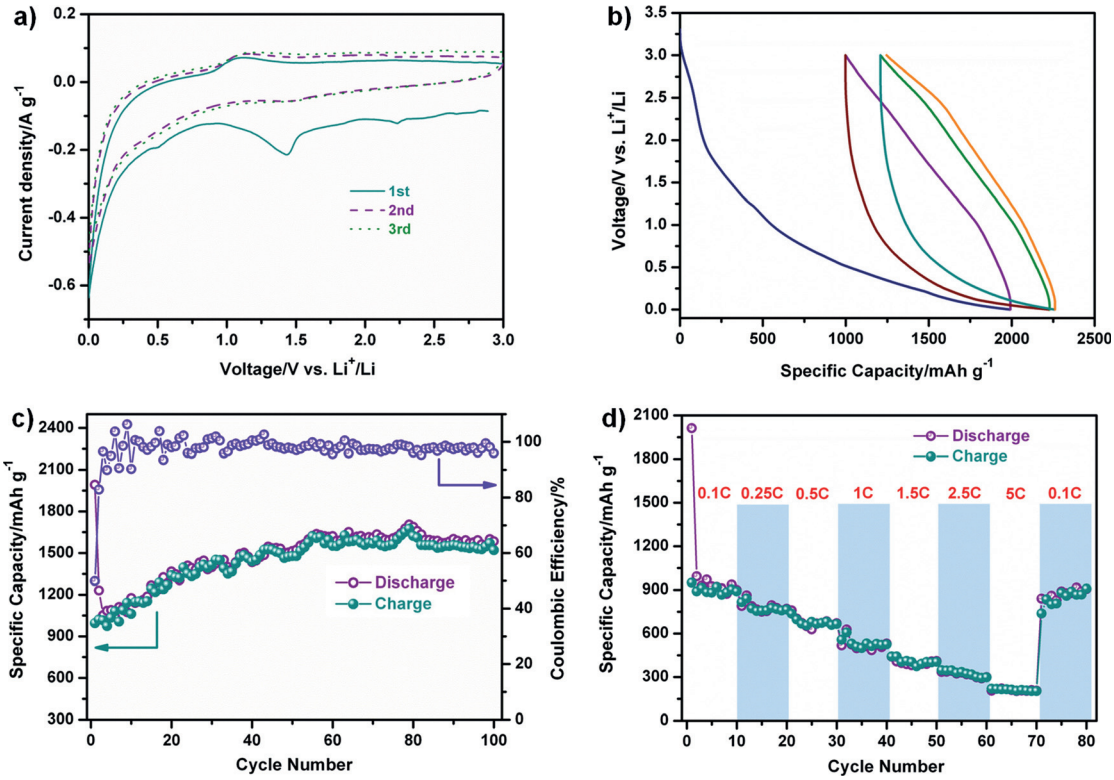

Figure 3. Electrochemical performance of PQL nanoparticles at ambient temperature. a) CV curves scanned at 0.1 mV s^{-1}. b) Galvanostatic discharge/charge profiles for the first three cycles at 100 mA g^{-1}. c) Cycling performance at 100 mA g^{-1}. d) Rate capability.

reversibility of PQL nanoparticles. Figure 3b shows galvanostatic discharge/charge profiles of PQL nanoparticles for the first three cycles at a current density of 100 mA g^{-1} between 0.0 and 3.0 V. In the first discharge process (Li^+ intercalation), the potential sharply drops from open-circuit voltage (OCV) of 3.05 V to 2.1 V, followed by slowly tapering off to ca. 0.8 V and then to 0.0 V. Upon subsequent charging, a sloping curve is presented. Thus the observed electrochemical discharge/charge characteristics agree well with the CV behavior. The initial specific discharge and charge capacities reach 1992 and 995 mAh g^{-1}, respectively, with a Coulombic efficiency of 49.9%. The large capacity loss (997 mAh g^{-1}) is mainly attributed to irreversible reactions (e.g., decomposition of electrolyte) to form a SEI film, which is a common character for LIB anodes in the first cycle.[17] But, the reversibility of lithium insertion and extraction is found to be greatly enhanced in the subsequent second and third cycles, e.g., delivering 1231 (discharge) and 1020 mAh g^{-1} (charge) in the second cycle. Additionally, the PQL electrode demonstrates an outstanding capacity retention performance. The specific capacity versus cycle number was studied at a rate of 100 mA g^{-1} (Figure 3c). It shows a very interesting phenomenon, that is, a remarkable increase in the capacity upon cycling, which has rarely been observed in previous organic electrodes.[11,12,18] The capacity increase is probably due to: 1) slow activation of electrode materials with more reaction sites during cycling,[19] and/or 2) gradual interfacial lithium storage in nanostructured PQL.[20] After 100 cycles, both the discharge and charge capacities were sustained at around a large value of 1550 mAh g^{-1}, which is several times higher than any value reported for organics (e.g., 450 mAh g^{-1} for ellagic acid[21] and 400 mAh g^{-1} for polyparaphenylene[22]), and even superior to state-of-the-art metal-oxide anodes (e.g., 920 mAh g^{-1} for Fe_2O_3[23] and 950 mAh g^{-1} for Co_3O_4[24]).

The reversible capacity, 1550 mAh g^{-1}, is astonishingly high and corresponds to twelve lithium intercalations per unit formula of PQL monomer. This result clearly demonstrates a novel lithium storage mechanism that challenges the traditional model of only one Li being intercalated into each C_6 ring in graphite material (LiC_6, 372 mAh g^{-1}). As depicted in Scheme 2, besides possible electrochemical lithiation at four nitrogen centers of PQL (step I), we believe that a maximum of twelve Li ions may be added on the unsaturated carbons of C_6 rings by forming a Li_6/C_6 complex (step II), which has also been shown for some multiring aromatic compounds.[11,14] The use of usual characterization techniques (such as NMR spectroscopy, XPS, or PXRD) to understand the mechanism failed because of the extremely

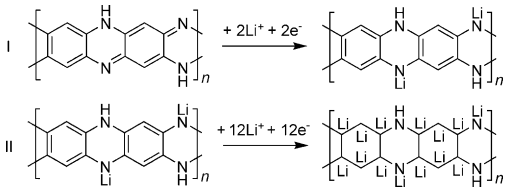

Scheme 2. Diagrams for the proposed electrochemical reactions of PQL.

poor solubility of the material, too broad peaks, and a poor crystallinity. To further understand our results, density functional theory (DFT) calculations with protonated azatetracene as a model were performed (Supporting Information). Our result (Figure S3) suggests that the stepwise insertion of Li ions into protonated azatetracene shows significant lower free energy than those of unsubstituted aromatics.[11] The result of calculations is also similar to previous results using multiring aromatic compounds with carbonyl groups.[11] Based on the above assumption (overall 14 lithium insertion), the theoretical capacity of PQL is calculated to be 1822 mAh g^{-1}. Owing to the effect of kinetics (current density), the practical Li-ion insertion capability (1550 mAh g^{-1}, twelve lithium insertion) is slightly inferior to the theoretical values.

PQL shows a promising electronic conducting property (2.1×10^{-3} S cm^{-1}), an important factor to achieve expected high-C-rate performance, which not only decreases the impedance of the electrode, but also facilitates the electron transfer inside the material. The cycling response of PQL nanoparticles at different C rates (each sustained for ten cycles) is illustrated in Figure 3c. A rate of *n*C is defined as a full charge/discharge of the theoretical capacity in 1/*n* hour. Here, 1 C equals a current density of 1822 mA g^{-1}. As seen from Figure 3c, the electrode can deliver specific discharge capacities of 890, 765, 666, 525, 405, 298, and 203 mAh g^{-1} during the 10th cycle at current rates of 0.1, 0.25, 0.5, 1, 1.5, 2.5, and 5 C, respectively. When the current density returns to 0.1 C, the capacity is able to immediately recover to its initial capacity. Moreover, the discharge/charge profiles at various rates during the 10th cycle were also drawn (Figure S4); and the contour of voltage versus capacity curve obtained at higher current rates is very similar to that at the low rate of 0.1 C, suggesting an insignificant polarization.

Since PQL shows a reasonable thermal stability up to 400 °C (Figure S2), the electrochemical activities of PQL nanoparticles at a high operating temperature of 50 °C were explored. As revealed by electrochemical impedance spectra (EIS) in Figure S5a, the lithiation kinetics of electrochemical reactions in the PQL electrode are enhanced remarkably at 50 °C. According to our simulations (Figure S5b and Table S1), the charge-transfer resistance (R_{ct}) at 50 °C is found to be about 105 Ω, whereas that at ambient temperature has a higher value of 175 Ω. Higher charge-transfer rates are favorable to reach higher capacity and superior rate capability at 50 °C (Figures 4 and S6–S8). The galvanostatic discharge/charge profiles (current density: 100 mA g^{-1}, 0.05 C) at 50 °C shown in Figure S6 are very similar to those obtained at ambient temperature (Figure 3b), undergoing similar redox reactions. As predicted, more lithium ions are reversibly stored in PQL molecules. At 50 °C, the electrode offers specific discharge and charge capacities of 2404 and 1140 mAh g^{-1} in the first cycle, respectively. In the second cycle, the lithium uptake and removal are highly reversible, showing discharge and charge capacities of 1249 and 1146 mAh g^{-1}, respectively. During 100 cycles (Figure S7), the capacity is gradually increased and finally sustained at around 1770 mAh g^{-1}, corresponding to 13.6 Li per unit formula, which comes closer to the theoretical values

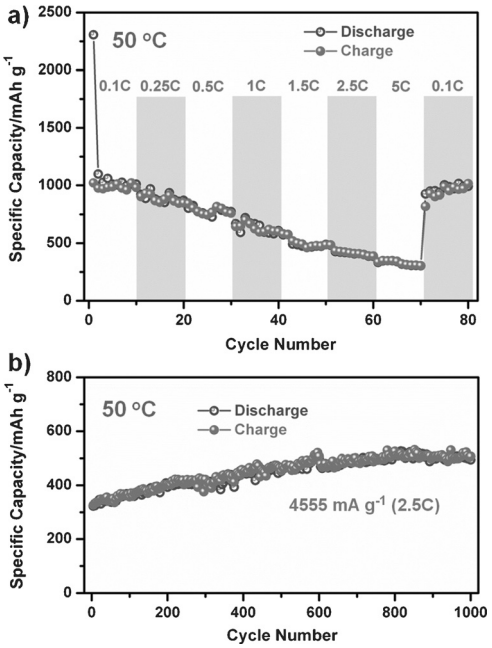

Figure 4. Electrochemical performance of PQL nanoparticles at 50 °C. a) Rate capability. b) Long-term cycling performance at a high rate of 4555 mA g^{-1} (2.5 C).

(1822 mAh g^{-1}, insertion of 14 lithium) compared to the ones at ambient temperature. Furthermore, the rate performance of PQL at 50 °C was also investigated (Figures 4a and S8). It can be seen that at current rates of 0.1, 0.25, 0.5, 1, and 1.5 C, Li ion insertion capacities during the 10th cycle are found to be 1010, 869, 775, 609, and 489 mAh g^{-1}, respectively. Surprisingly, even at higher rates of 2.5 and 5 C, reversible capacities of 385 and 303 mAh g^{-1}, respectively, can still be obtained. More surprisingly, as shown in Figure 4b, the PQL electrode can be successfully cycled for 1000 times under a high temperature of 50 °C and a high rate of 2.5 C (4555 mA g^{-1}). Analogous to the cycling behavior at low current (Figures 3c and S7), the specific capacity is increased upon repeated lithium uptake/removal, and stabilized at around 500 mAh g^{-1} after 1000 cycles, indicating a high and fast accessibility for lithium insertion/extraction into/from PQL. To the best of our knowledge, such cycling performance in terms of long lifecycle (1000 cycles), high capacity (500 mAh g^{-1}), high rate (4555 mA g^{-1}), and high operating temperature (50 °C) is the best performance among the organic-molecule-based anode materials reported so far,[5c] and even superior to some of the state-of-the-art inorganic metal-oxide active materials (see Table S2). In comparison, the electrochemical activities of PQL nanoparticles at low operating temperature were also explored (Figures S9 and S10) and the capacity of PQL at 0 and −20 °C are 352 and 108 mAh g^{-1}, respectively. The poor electrochemical performance might be due to low lithiation insertion into the PQL electrode and the restricted charge transfer of electrolyte at low temperature.

In conclusion, the nanoparticles of PQL have been prepared by using a reprecipitation method. The as-prepared

ladder polymer PQL nanoparticles show high performance as anode materials in LIBs, not only at room temperature but also at high operating temperature (50 °C). For example, at 50 °C, PQL can achieve a high reversible capacity of 1770 mAh g^{-1} at a low rate of 0.05 C, and deliver a capacity of 303 mAh g^{-1} at a high rate of 5 C, and even sustain a capacity of 500 mAh g^{-1} after 1000 charge/discharge cycles at a rate of 2.5 C. Our results show that conjugated ladder polymer nanostructures, which containing a high number of nitrogen heteroatoms, could be promising candidates for organic anode materials.

Keywords: anode materials · electrochemistry · ladder polymers · lithium batteries · polyazaacene analogues

How to cite: *Angew. Chem. Int. Ed.* **2015**, *54*, 7354–7358
Angew. Chem. **2015**, *127*, 7462–7466

[1] a) J. M. Tarascon, M. Armand, *Nature* **2001**, *414*, 359–367; b) M. Armand, J. M. Tarascon, *Nature* **2008**, *451*, 652–657.
[2] a) J.-M. Tarascon, *Nat. Chem.* **2010**, *2*, 510–510; b) P. Poizot, F. Dolhem, *Energy Environ. Sci.* **2011**, *4*, 2003–2019; c) L.-X. Yuan, Z.-H. Wang, W.-X. Zhang, X.-L. Hu, J.-T. Chen, Y.-H. Huang, J. B. Goodenough, *Energy Environ. Sci.* **2011**, *4*, 269–284.
[3] a) D. Larcher, J. M. Tarascon, *Nat. Chem.* **2015**, *7*, 19–29; b) M.-S. Balogun, W. Qiu, W. Wang, P. Fang, X. Lu, Y. Tong, *J. Mater. Chem. A* **2015**, *3*, 1364–1387; c) X. Rui, H. Tan, Q. Yan, *Nanoscale* **2014**, *6*, 9889–9924.
[4] L. Ji, Z. Lin, M. Alcoutlabi, X. Zhang, *Energy Environ. Sci.* **2011**, *4*, 2682–2699.
[5] a) F. Cheng, J. Liang, Z. Tao, J. Chen, *Adv. Mater.* **2011**, *23*, 1695–1715; b) Y. Liang, Z. Tao, J. Chen, *Adv. Energy Mater.* **2012**, *2*, 742–769; c) Z. Song, H. Zhou, *Energy Environ. Sci.* **2013**, *6*, 2280–2301.
[6] N. Oyama, J. M. Pope, T. Sotomura, *J. Electrochem. Soc.* **1997**, *144*, L47–L51.
[7] a) K. Oyaizu, H. Nishide, *Adv. Mater.* **2009**, *21*, 2339–2344; b) T. Janoschka, M. D. Hager, U. S. Schubert, *Adv. Mater.* **2012**, *24*, 6397–6409.
[8] a) N. Oyama, T. Tatsuma, T. Sato, T. Sotomura, *Nature* **1995**, *373*, 598–600; b) L. Zhan, Z. Song, J. Zhang, J. Tang, H. Zhan, Y. Zhou, C. Zhan, *Electrochim. Acta* **2008**, *53*, 8319–8323.
[9] a) L. Zhao, J. Zhao, Y.-S. Hu, H. Li, Z. Zhou, M. Armand, L. Chen, *Adv. Energy Mater.* **2012**, *2*, 962–965; b) S. Wang, L. Wang, K. Zhang, Z. Zhu, Z. Tao, J. Chen, *Nano Lett.* **2013**, *13*, 4404–4409; c) S. Wang, L. Wang, Z. Zhu, Z. Hu, Q. Zhao, J. Chen, *Angew. Chem. Int. Ed.* **2014**, *53*, 5892–5896; *Angew. Chem.* **2014**, *126*, 6002–6006.
[10] a) A. Abouimrane, W. Weng, H. Eltayeb, Y. Cui, J. Niklas, O. Poluektov, K. Amine, *Energy Environ. Sci.* **2012**, *5*, 9632–9638; b) W. Huang, Z. Zhu, L. Wang, S. Wang, H. Li, Z. Tao, J. Shi, L. Guan, J. Chen, *Angew. Chem. Int. Ed.* **2013**, *52*, 9162–9166; *Angew. Chem.* **2013**, *125*, 9332–9336; c) W. Luo, M. Allen, V. Raju, X. Ji, *Adv. Energy Mater.* **2014**, *4*, 1400554; d) H.-g. Wang, S. Yuan, D.-l. Ma, X.-l. Huang, F.-l. Meng, X.-B. Zhang, *Adv. Energy Mater.* **2014**, *4*, 1301651; e) Z. Zhu, M. Hong, D. Guo, J. Shi, Z. Tao, J. Chen, *J. Am. Chem. Soc.* **2014**, *136*, 16461–16464.
[11] X. Han, G. Qing, J. Sun, T. Sun, *Angew. Chem. Int. Ed.* **2012**, *51*, 5147–5151; *Angew. Chem.* **2012**, *124*, 5237–5241.
[12] a) X. Han, C. Chang, L. Yuan, T. Sun, J. Sun, *Adv. Mater.* **2007**, *19*, 1616–1621; b) K. Sakaushi, G. Nickerl, F. M. Wisser, D. Nishio-Hamane, E. Hosono, H. Zhou, S. Kaskel, J. Eckert, *Angew. Chem. Int. Ed.* **2012**, *51*, 7850–7854; *Angew. Chem.* **2012**, *124*, 7972–7976.
[13] a) C. Wang, J. Zhang, G. Long, N. Aratani, H. Yamada, Y. Zhao, Q. Zhang, *Angew. Chem. Int. Ed.* **2015**, DOI: 10.1002/anie.201500972; *Angew. Chem.* **2015**, DOI: 10.1002/ange.201500972; b) J. Li, P. Li, J. Wu, J. Gao, W. Xiong, G. Zhang, Y. Zhao, Q. Zhang, *J. Org. Chem.* **2014**, *79*, 4438; c) C. Wang, J. Wang, P. Li, J. Gao, S. Y. Tan, W. Xiong, B. Hu, P. S. Lee, Y. Zhao, Q. Zhang, *Chem. Asian J.* **2014**, *9*, 779; d) P.-Y. Gu, F. Zhou, J. Gao, G. Li, C. Wang, Q.-F. Xu, Q. Zhang, J.-M. Lu, *J. Am. Chem. Soc.* **2013**, *135*, 14086; e) G. Li, H. M. Duong, Z. H. Zhang, J. C. Xiao, L. Liu, Y. L. Zhao, H. Zhang, F. W. Huo, S. Z. Li, J. Ma, F. Wudl, Q. C. Zhang, *Chem. Commun.* **2012**, *48*, 5974–5976; f) G. Li, K. Zheng, C. Y. Wang, K. S. Leck, F. Z. Hu, X. W. Sun, Q. C. Zhang, *ACS Appl. Mater. Interfaces* **2013**, *5*, 6458–6462; g) G. Li, Y. C. Wu, J. K. Gao, J. B. Li, Y. Zhao, Q. C. Zhang, *Chem. Asian J.* **2013**, *8*, 1574–1578; h) G. Li, Y. C. Wu, J. K. Gao, C. Y. Wang, J. B. Li, H. C. Zhang, Y. Zhao, Y. L. Zhao, Q. Zhang, *J. Am. Chem. Soc.* **2012**, *134*, 20298–20301.
[14] J. Wu, X. Rui, C. Wang, W.-B. Pei, R. Lau, Q. Yan, Q. Zhang, *Adv. Energy. Mater.* **2015**, DOI: 10.1002/aenm.201402189.
[15] a) J. K. Stille, E. L. Mainen, *Macromolecules* **1968**, *1*, 36–42; b) S. Y. Hong, M. Kertesz, Y. S. Lee, O. K. Kim, *Chem. Mater.* **1992**, *4*, 378–383.
[16] K. Chiba, T. Ohsaka, Y. Ohnuki, N. Oyama, *J. Electroanal. Chem. Interfacial Electrochem.* **1987**, *219*, 117–124.
[17] D. Hao Sim, X. Rui, J. Chen, H. Tan, T. M. Lim, R. Yazami, H. H. Hng, Q. Yan, *RSC Adv.* **2012**, *2*, 3630–3633.
[18] a) W. Walker, S. Grugeon, O. Mentre, S. Laruelle, J.-M. Tarascon, F. Wudl, *J. Am. Chem. Soc.* **2010**, *132*, 6517–6523; b) J. Hong, M. Lee, B. Lee, D.-H. Seo, C. B. Park, K. Kang, *Nat. Commun.* **2014**, *5*, 5335.
[19] J. Liu, D. Qian, H. Feng, J. Li, J. Jiang, S. Penga, Y. Liu, *J. Mater. Chem. A* **2014**, *2*, 11372–11381.
[20] N. A. Kaskhedikar, J. Maier, *Adv. Mater.* **2009**, *21*, 2664–2680.
[21] S. Goriparti, M. N. K. Harish, S. Sampath, *Chem. Commun.* **2013**, *49*, 7234–7236.
[22] L. M. Zhu, A. W. Lei, Y. L. Cao, X. P. Ai, H. X. Yang, *Chem. Commun.* **2013**, *49*, 567–569.
[23] J. Zhu, Z. Yin, D. Yang, T. Sun, H. Yu, H. E. Hoster, H. H. Hng, H. Zhang, Q. Yan, *Energy Environ. Sci.* **2013**, *6*, 987–993.
[24] X. Rui, H. Tan, D. Sim, W. Liu, C. Xu, H. H. Hng, R. Yazami, T. M. Lim, Q. Yan, *J. Power Sources* **2013**, *222*, 97–102.

Received: April 2, 2015
Published online: May 8, 2015

